

WIDE RUNNING CONTROL INTEGRATED BANG-BANG CONTROL WITH REGULATORY CONTROL: STRATEGY, APPROACH AND PERFORMANCE

XIONGLIN LUO AND MINGJUN LI

Department of Automation
China University of Petroleum – Beijing
No. 18, Fuxue Road, Changping District, Beijing 102249, P. R. China
luoxl@cup.edu.cn; ljmuma@outlook.com

Received January 2016; revised May 2016

ABSTRACT. *Regulatory proportional-integral-derivative control remains dominant in actual industrial processes. Regulatory proportional-integral-derivative control is adaptable and easy to use and has a simple principle and strong robustness. It can meet the control requirement within a certain scope of changes. However, it can hardly regulate both overshoot and conditioning time in the case of wide running condition changes. Wide running control-integrated Bang-Bang control with regulatory control is used as a complementary strategy in this study. The phase locus graphic method is adopted to compute the switch point of the Bang-Bang control. The influence of the measurement error of the switch point on the control process is discussed, and the complementary characteristics of wide running control and regulatory control are analyzed. Given different objects, two computing solutions are given to determine and select whether wide running control or regulatory control is the better option. Simulation reveals that the integrated control strategy with wide running control, can handle the problem of excessive overshoot or conditioning time and wide running control is a flexible and effective complement to regulatory control.*

Keywords: Wide running control, Bang-Bang control, Control design, Nonlinear system, Starting threshold

1. Introduction. Despite the various advanced control methods that have continuously emerged in the past decades, the regulatory proportional-integral-derivative (PID) control remains most widely used in practical industrial areas. It has several strong points, such as its simple structure, easy implementation and robust operation. However, when wide running changes occur, such as the start-up process, a satisfactory result may not be obtained using the traditional PID control. The deterioration of the control process affects the economic efficiency and production safety of enterprises. Therefore, PID control should be improved to meet the entire range of working condition changes.

It is generally considered that, if the overshoot is within a reasonable range, then the less the duration time is, the lower the cost of the switching process [1] is. Bang-Bang control proposed by Pontryagin, especially the strategy integrated in the Bang-Bang control and PID control, is widely used to solve time optimization problems [2-5]. When a new set of point value arrives, the strategy chooses Bang-Bang control to reduce the error between the new set of point value and controlled variable in a short period of time. When the error is smaller than the prescribed limit, the strategy employs PID control to eliminate the steady-state error and accomplish the whole control process. This strategy is an effective improvement of the regulatory PID control. The two control methods combine each other's advantages and compensate for each other's deficiencies. However, Bang-Bang control has rather strict requirements for the switch point. In addition to the

switching between the maximum and minimum control signals, another switch point is required between the Bang-Bang control and PID control. Both switch points should be taken seriously; otherwise, they can result in the disorder of the whole control process.

The calculation of the switch value or moment in nonlinear systems continues to be a difficult issue. The problems in the analytical form are difficult to solve. Thus, the study and application of numerical solutions have become increasingly extensive. Many emerging methods are available, some of which have already made their marks, whereas the others have not. Nevertheless, any method has its own advantages as well as shortcomings. Kaya and Noakes proposed two types of optimization methods based on derivatives: switch time computation (STC) and time optimal switching (TOS) [6,7]. However, the computation processes of these methods are complicated. Luo et al. [8] used velocity error accumulated method to design a temperature velocity controller. According to the object model, temperature inertia monitoring was used to predict the switching point of temperature control and its velocity control. However, uniform velocity heating weakened the thermal inertia and sacrificed regulation time. Then for time optimal control, Luo et al. [9] converted the modified switch control problems into nonlinear programming problems, produced a generic calculation method and added a buffer stage to improve the control performance within an inaccurate switch point. Xiao [10] combined the PID control with a neural network and utilized expert experience to judge the timing of the switch. However, the said study was limited in terms of the experience of the control schemes. Zhou and Zhao [11] designed a particle swarm optimization algorithm to solve the Bang-Bang optimal control problem, in which the entire time interval was divided into subintervals with varying lengths that were treated as variables. However, the solution time was not controllable for online application. Ping and Luo [12] approximately used several first order linear transfer functions to calculate the switch point of a multi-model control strategy. However, the computational accuracy is not high. Ke and Gao [13] analyzed the fastest heating process of a heating furnace and showed that the switch point should be the intersection of the state curves of the full-on and full-off state. Nevertheless, the specific calculation method of the intersection was not mentioned.

The primary contributions of this essay are twofold. The first point is a new computing method of the switch point of Bang-Bang control. Before the control scheme can work, the judgment module incorporated in it selects between the two control methods according to the changes in the set value. The switch point of Bang-Bang control and the analysis of the selection of the control method are based on the phase locus graphic method. This method has the advantages of time controllability, high precision and online applicability.

No comprehensive precedent exists in the related literature for the comparison of Bang-Bang control and PID control. The second contribution is to analyze their advantages and disadvantages from a brand new perspective. On the one hand, PID control is currently rather mature in the industrial fields. Other methods should not be used if PID control can achieve satisfactory results. On the other hand, Bang-Bang control requires a high-precision switching action to achieve a rapid dynamic performance. A minimal error in the switch point may cause significant deterioration. Based on the above consideration, the selection between Bang-Bang control and PID control is determined in this study by analyzing the measurement error of the controlled variable. Two calculation methods for the selective conditions – online and offline methods – are designed for different objects.

The structure of the present study is divided into three parts: strategy, approach and performance. In Section 2, we propose the reasons why a satisfactory result may not be obtained by the regulatory control, and then provide an overview of our control strategy including the control structure, principle and difficulties. Sections 3 to 4 analyze the two key difficulties to approach the control strategy and produce new computing methods

to solve the key difficulties from different angles which were never considered in other literature. The simulation in Section 5 reveals that the integrated control strategy is much better than any single traditional control method. Conclusions are made in Section 6.

2. Wide Running Control. The reasons for the inefficient performance of regulatory control under wide condition changes are as follows. Firstly, for general processes, the regulation time and the overshoot are contradictory. Less regulation time means more overshoot. Secondly, the overshoot is in theory a fixed percentage in a linear system. Its absolute value increases with an increase in the difference between the set value and initial value. The same condition holds true in nonlinear systems. Finally, the optimal PID parameters are difficult to obtain all the time through online parameter tuning. As shown in Figure 1, if only slight changes occur in the set point value, then Bang-Bang control and PID control have a similar performance. When a large variation occurs, Bang-Bang control is ideally much better than the problem-prone PID control.

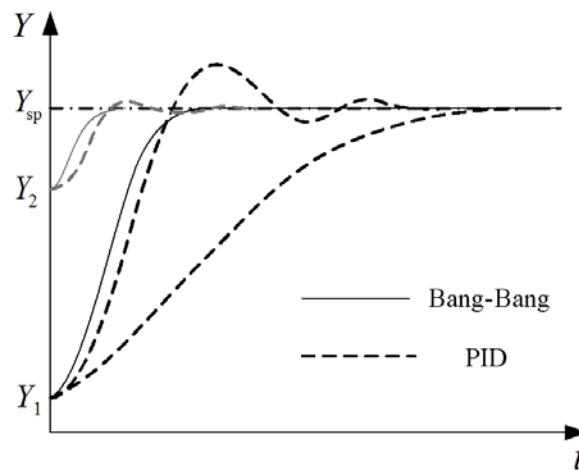


FIGURE 1. Comparison between Bang-Bang control and PID control

The control strategy in the present study employs wide running control (WRC)-integrated Bang-Bang control with regulatory control to address a wide range of changes in the set value. Proportional-integral (PI) control is used as the regulatory control to handle the smaller ones. The flow chart is shown in Figure 2 and the structure with two switch points is shown in Figure 3.

Figure 2 shows that Bang-Bang control complements regulatory control and that regulatory control is the last step of WRC. Figure 3 shows that, when the new set value Y_{sp} arrives, the switching judgment module calculates the deviation e_2 between Y_{sp} and the controlled variable Y . The module then selects regulatory control or WRC through switch point P_2 . If WRC starts, then the maximum input u_{max} acts on the object. When Y is close to Y_{sw} , the input value is changed to the minimum u_{min} through the switch point P_1 . When Y is close to Y_{sp} , the strategy switches to regulatory control to eliminate the small deviation through the switch point P_2 and then accomplishes the entire control process.

Two elements are key to the integrated control strategy: the first one is the switch value of Bang-Bang control, the second one is the selection judgment of the two control methods, that is, judging whether the variation of the set value is large or small enough.

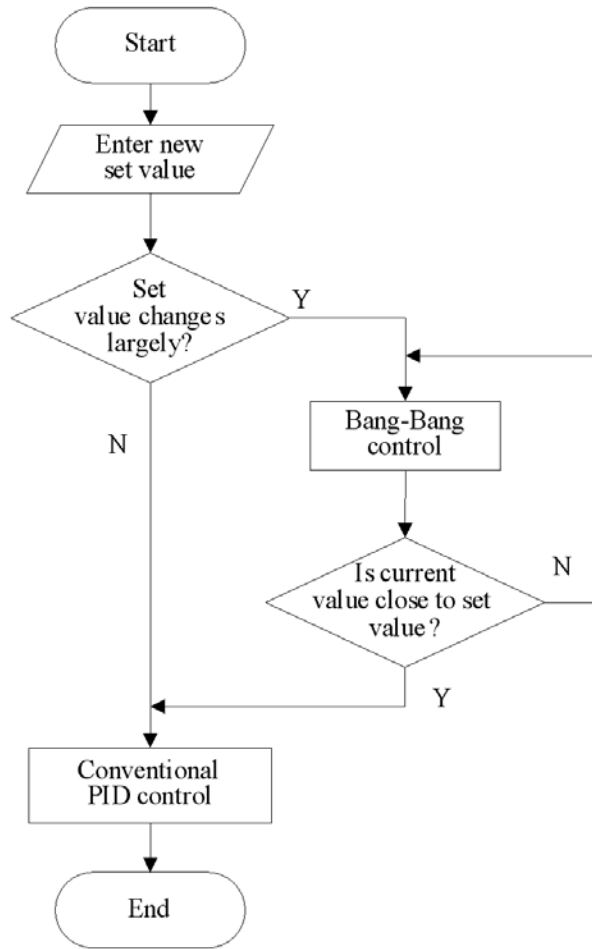
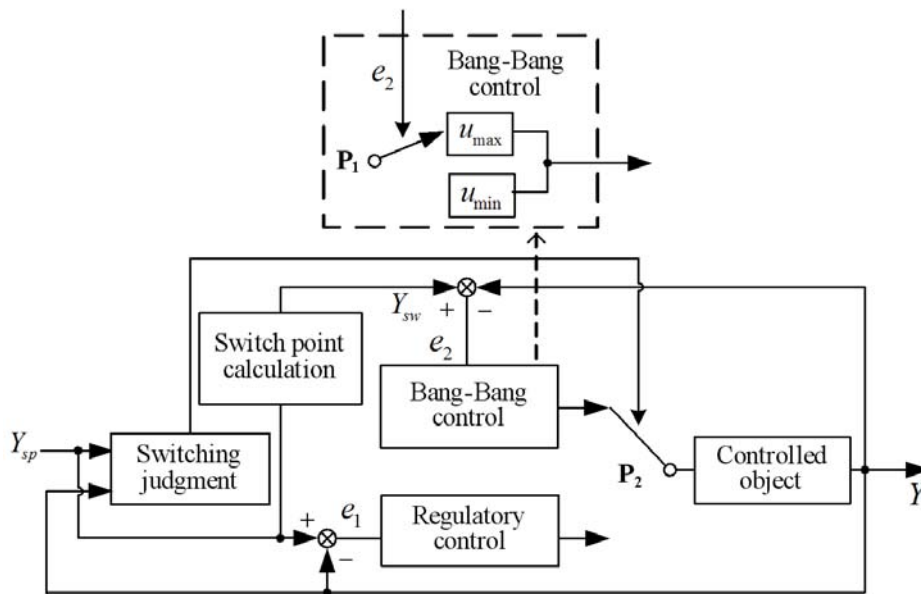


FIGURE 2. Flow chart of WRC



Note: P_1 and P_2 are the switch points

FIGURE 3. Structure chart of WRC

3. Calculation of the Switch Point of Bang-Bang Control. For the time optimal problem of the single-input-single-output (SISO) linear time-invariant system, the principle of minimum can be applied to obtaining a group of phase path trajectories. The unique trajectory is easily identifiable with the known initial status and final status. When the number of switch action is one, the optimal control switch point must be the intersection of two curves determined by the maximum and minimum input values. Extending this idea to nonlinear systems, if we can obtain the optimal phase path trajectories that satisfy the given status, then the intersection is the optimal switch point of Bang-Bang control.

Taking a stable second-order nonlinear system as an example, the system equations can be expressed as follows:

$$\dot{x}_1(t) \equiv \frac{dx_1(t)}{dt} = f_1(x_1(t), x_2(t), u(t)) \tag{1}$$

$$\dot{x}_2(t) \equiv \frac{dx_2(t)}{dt} = f_2(x_1(t), x_2(t), u(t)) \tag{2}$$

$$\text{initial conditions: } x_0 = [x_1^0, x_2^0]$$

$$\text{terminal conditions: } x_T = [x_{1T}, x_{2T}]$$

x_1, x_2 are the two state variables and u is the input variable of the state equations. f_1 and f_2 are the general expressions of the state equations.

Assuming the input is the maximum before the switch moment t_{sw} , and then minimum.

$$\text{input value: } \begin{cases} u_{\max} & t < t_{sw} \\ u_{\min} & t \geq t_{sw} \end{cases}$$

Assuming $f_2(t, x_1(t), x_2(t), u(t)) \neq 0$, by transferring Equation (2) and eliminating dt in Equation (1), we obtain

$$\frac{dx_1(t)}{dx_2(t)} = \frac{f_1(x_1(t), x_2(t), u(t))}{f_2(x_1(t), x_2(t), u(t))} \tag{3}$$

Substituting the maximum and minimum input values in Equation (3),

$$F_1(x_1(t), x_2(t)) = \frac{f_1(x_1(t), x_2(t), u_{\max})}{f_2(x_1(t), x_2(t), u_{\max})} \tag{4}$$

$$F_1(x_1(t), x_2(t)) = \frac{f_1(x_1(t), x_2(t), u_{\min})}{f_2(x_1(t), x_2(t), u_{\min})} \tag{5}$$

The first phase curve L_1 , as shown in Figure 4, can be obtained using a numerical solution to solve Equation (4), with x_0 as the initial conditions. However, the initial conditions of Equation (5) are unknown, and the initial conditions themselves are the switch values that we aim to obtain. Under this circumstance, the numerical solution, taking the Eulerian method as an example here, needs adjustment.

Taking the terminal conditions as the new initial conditions of discrete calculation:

$$[x_1^*(0), x_2^*(0)] = [x_{1T}, x_{2T}]$$

The Eulerian method can be represented as

$$\begin{aligned} x_2^*(i+1) &= x_2^*(i) + t_{step} \\ x_1^*(i+1) &= x_1^*(i) + F_2(x_1^*(i), x_2^*(i)) \cdot t_{step} \end{aligned} \tag{6}$$

where t_{step} is the calculation step. x_1^* and x_2^* are the new state variables. One-to-one correspondences exist between the inverse solutions and the original solutions:

$$\begin{aligned} x_2(n-i-1) &= x_2^*(i+1) \\ x_1(n-i-1) &= x_1^*(i+1) \\ x_2(n) &= x_{1T} \\ x_1(n) &= x_{2T} \end{aligned} \tag{7}$$

where $i = 0, 1, 2, \dots, n - 1$; $n = \frac{t_f}{t_{step}}$; and t_f is the terminal moment. The second phase curve L_2 in Figure 4 consists of $[x_1, x_2]$, instead of $[x_1^*, x_2^*]$.

The key to the inverse solutions is approximately replacing $F_2(x_1(i - 1), x_2(i - 1))$ with $F_2(x_1(i), x_2(i))$. After verification, the inverse solutions can meet the precision requirement within a sufficiently small calculation step.

The intersection of L_1 and L_2 is the optimal switch point of Bang-Bang control. Similarly, the reverse process can be obtained using the original state as the starting point and the original initial state as the end point. The phase trajectory curves of the reverse process are L_3 and L_4 in Figure 4.

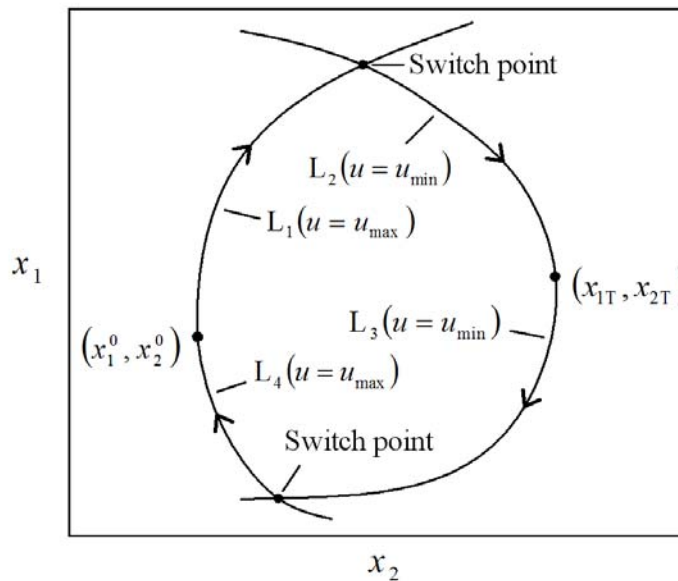


FIGURE 4. Diagram of the phase locus graphic method

3.1. The van der Pol equation. The classical van der Pol equation [7] is given in a phase-variable form

$$\begin{cases} \dot{x}_1 = x_2 \\ \dot{x}_2 = -x_1 - (x_1^2 - 1)x_2 + u \end{cases}$$

The initial and target points are given as $x_0 = [1, 1]$ and $x_T = [0, 0]$, respectively. It should be noticed that the equation $F \equiv dx_2/dx_1$ needs a nonzero denominator. The target point $x_T = [0, 0]$ cannot meet this demand. To avoid the situation of a non-existent solution, we replace it with $x'_T = [0, \sigma]$, where $\sigma \rightarrow 0^-$.

The phase locus curves are shown in Figure 5. The coordinate of the intersection is (1.13851, -0.58663). The corresponding switch moment is $t_s = 0.7109$ s. Compared with the optimisation result in [7], the error is approximately 1.67%.

3.2. Laboratory electric heating furnace. The second object is based on the electric heating furnace in our laboratory [8].

In [8], the electric heating furnace model was not used as the primary case study but only as an example to analyze the capability of the control system. We improve the model into a second-order nonlinear system to accurately describe the time-delay and

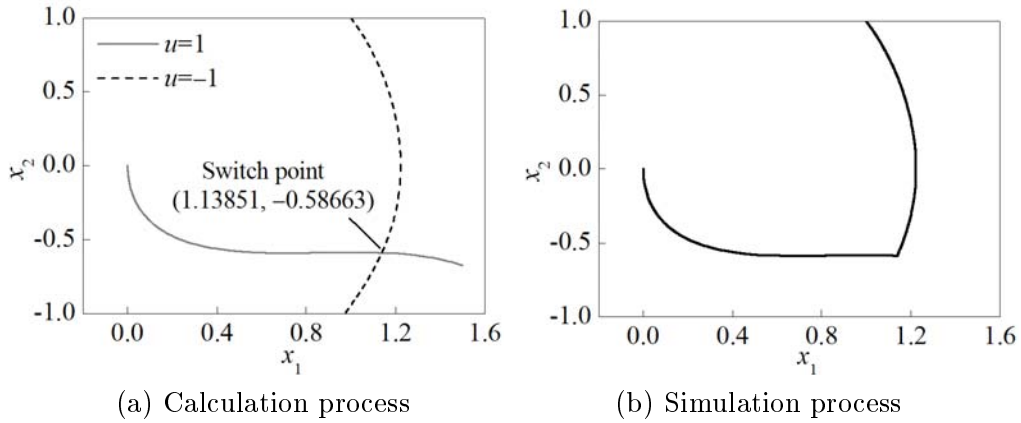


FIGURE 5. Phase locus and switch points of the van der Pol equation



FIGURE 6. Electric heating furnace in our laboratory



FIGURE 7. Internal structure of the electric heating furnace

asymmetric characteristic of the nonlinear system. The equations are as follows:

$$\left[108.9 - 10(T - 755)^{\frac{2}{7}} \right] \frac{dT}{dt} + 0.3214(T - T_{\text{atm}})^{\frac{5}{4}} = \omega$$

$$3.00 \frac{d\omega}{dt} + \omega = 0.0835U^2$$

where T is the internal temperature of heating furnace, T_{atm} is the atmospheric temperature, U is the input voltage and ω is the intermediate variable meaning the effect of input voltage.

The whole process is divided into four stages. The full-heating state with input voltage $U_{\text{max}} = 220$ V, the self-heating state with $U_{\text{min}} = 0$ V, the self-cooling state with $U_{\text{min}} = 0$ V and the full-cooling state with $U_{\text{max}} = 220$ V. The phase locus curves for a cyclic process in the temperature from 400 °C to 500 °C are plotted in Figure 8(a). The curve L_5 consists of the steady-state operating points of the electric heating furnace model. The starting point and ending point of an arbitrary heating or cooling process must lie in this line and so are the point A and C. The coordinate of the intersection point B and D are (451.22, 2560.71) and (401.96, 12.84). The switch temperature of heating process is 451.22 °C, and the switch moment is 4.56 min. Compared with the optimal result of 4.5403 min in [8], the error is approximately 0.4%. The switch temperature of cooling process is 401.96 °C. When the temperature is close to 401.96 °C, U_{max} starts to affect the object. After 27 s, the temperature reaches the set value. Compared to the heating process, the duration of the buffer stage is very short. This fully reflects the asymmetry of the dynamic response of the heating furnace.

4. Selection and Judgment between Starting WRC or Regulatory Control.

When the new set value arrives, the judgment module determines which control method should be started by comparing their performance. WRC is designed as the additional method to meet the requirements of wide running condition changes. Therefore, the wide running condition change is necessary to be identified.

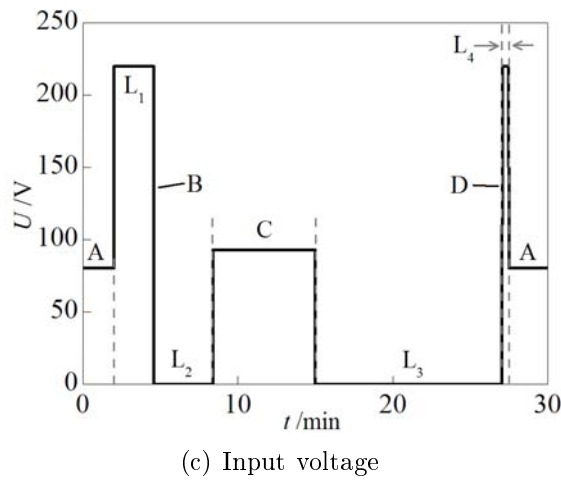
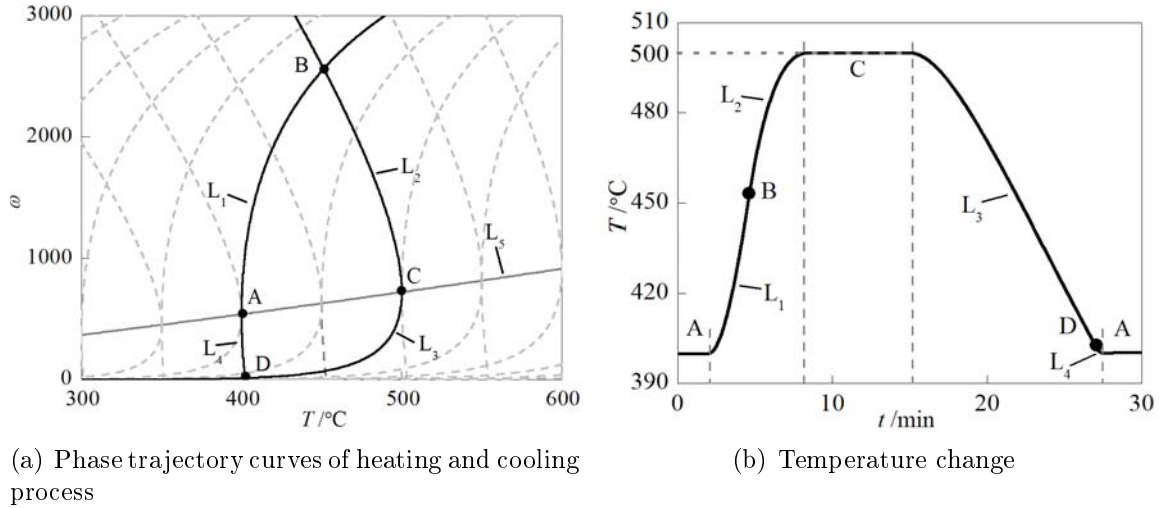
As we all know, PID control is difficult to quantitatively analyze for an arbitrary non-linear system. Accordingly, we convert ideas. By analyzing the shortcomings of WRC, we develop a method to calculate the starting threshold of WRC.

4.1. Effect of the temperature measurement error on the control process. Bang-Bang control has a great advantage in terms of regulation time. Given that the input of Bang-Bang control is not related to the deviation of the set value, it always consists of the maximum and minimum values. However, a large input results in a rapid increase in temperature and also a large overshoot easily. Hence, accurate switch temperature and switch action are vital to avoid the overshoot. Nevertheless, the measuring system in a practical system is prone to produce unpredictable small errors. The effect caused by the measurement error must be considered.

Figure 9 shows an increase in the temperature from 195 °C to 200 °C. The curve L_2 is the ideal Bang-Bang control effect, and the curves L_1 and L_3 are caused by the inaccurate switch action with ± 0.1 °C errors (T_{error}). The overshoot of the curve L_1 is 0.86 °C. Before PI control starts, the maximum temperature of the curve L_3 is 0.88 °C lower than 200 °C. A measurement error of 0.1 °C can cause an overshoot of 0.86 °C, which is nearly four times larger than the optimal PI control, but their regulation time is approximately the same. Under this condition, WRC should therefore not be selected. Continue to contrast with a larger temperature difference ΔT_{sp} .

TABLE 1. Comparison of control effect with $\Delta T_{sp} = 10$ °C

$\Delta T_{sp} = 10$ °C	WRC	PI control
Overshoot	0.69 °C	0.44 °C
Regulation time (5%)	9.29 min	11.38 min



Note: L_1 is the full-heating process, L_2 is the self-heating process, L_3 is the self-cooling process, L_4 is the full-cooling process, Point A is steady-state operating point of 400 °C, Point C is steady-state operating point of 500 °C, Point B is the switch point of heating process, and Point D is the switch point of cooling process.

FIGURE 8. Control effect of the heating furnace model

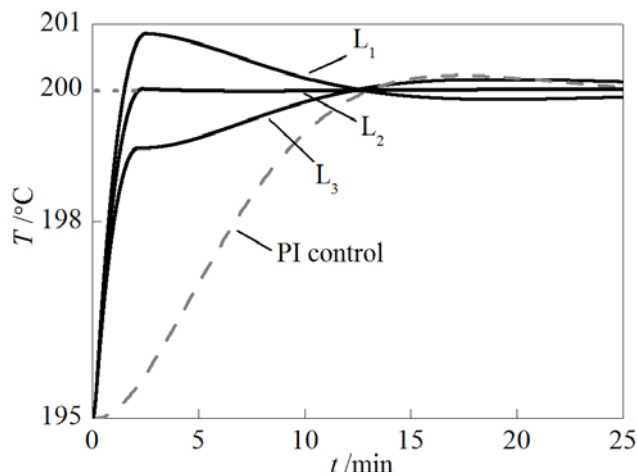
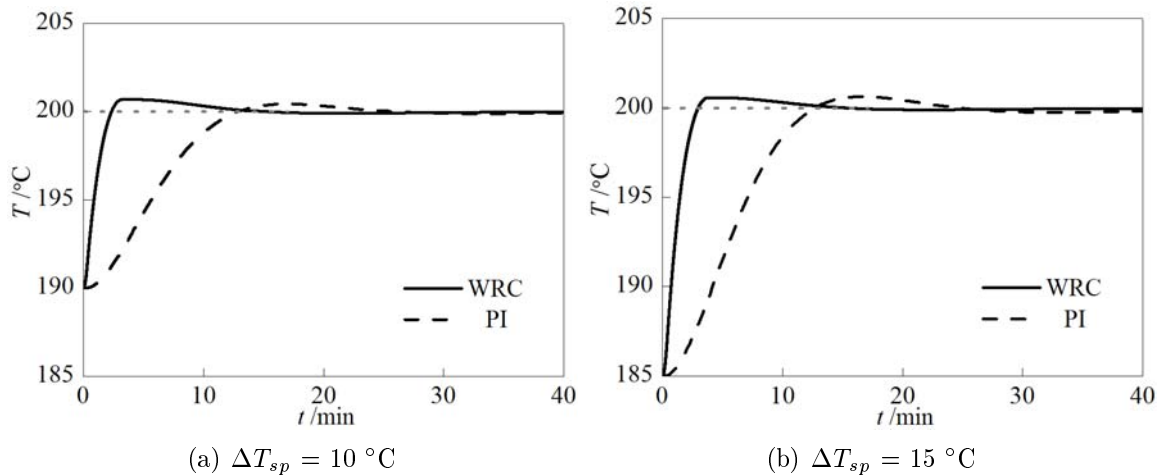


FIGURE 9. Comparison of different control effects ($\Delta T_{sp} = 5\text{ }^\circ\text{C}$)

FIGURE 10. Control performances with different ΔT_{sp} TABLE 2. Comparison of control effect with $\Delta T_{sp} = 15\text{ }^{\circ}\text{C}$

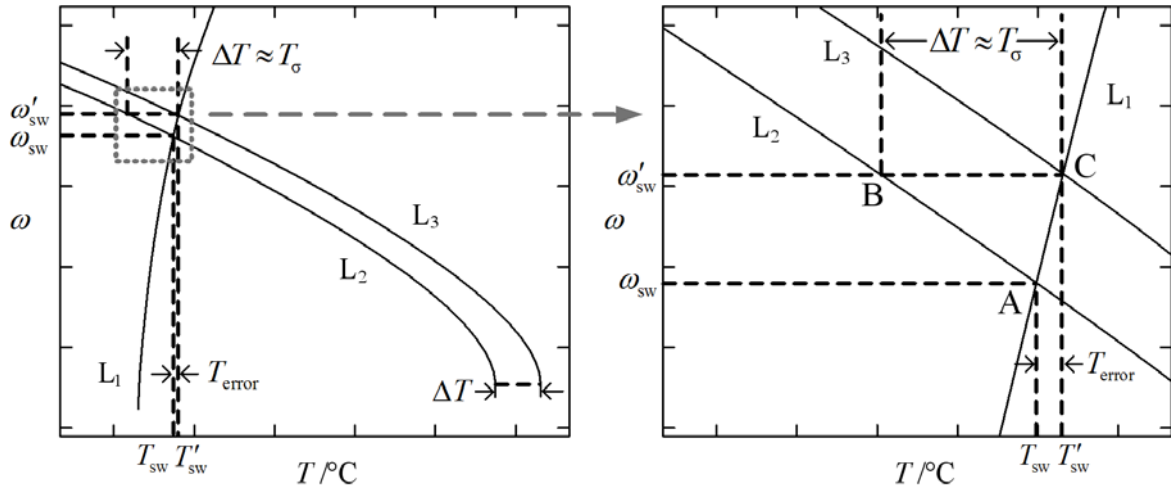
$\Delta T_{sp} = 15\text{ }^{\circ}\text{C}$	WRC	PI control
Overshoot	0.57 $^{\circ}\text{C}$	0.64 $^{\circ}\text{C}$
Regulation time (5%)	2.57 min	11.18 min

As shown above, the control performances of WRC and optimal PI control are approximately equal in the second case. However, when $\Delta T_{sp} = 15\text{ }^{\circ}\text{C}$, WRC has an obvious advantage. The overshoot in the third case does not exceed the allowed error band (5%), so that any adjustment of time makes no difference. Therefore, we may draw the conclusion that whether or not WRC can show its advantages depends on whether or not the absolute value of the overshoot caused by the measurement error is allowable.

4.2. Analysis and prediction of the overshoot caused by the temperature measurement error. Given the significant effects, the overshoot of WRC needs to be estimated in some way.

As Figure 11 shows, the phase curves of the full-heating and self-heating states are L_1 and L_2 , respectively. The point A (T_{sw}, ω_{sw}) is the intersection, that is, the calculation switch point. A new switch temperature is set as $T_{sw}^* = T_{sw} + T_{error}$. The corresponding switch point C (T_{sw}^*, ω_{sw}^*) is named the delay switch point. Translating L_2 to the right until point C is on it, we can generate a new curve L_3 that can approximately characterize the heating effect caused by the delay switch point. The variation in the value of the horizontal coordinate ΔT is approximately equal to the T_{σ} caused by the delay switch action. The overshoot of WRC resulting from the measurement error using the above method is predicable under the condition of given measurement error, initial temperature and terminal temperature. The principle of the method can be stated as follows. The variation trend of the solutions of nonlinear differential equations with similar initial conditions is approximately the same. Through numerical simulation and testing, the calculation error of this method is determined to be less than 1%.

The partial enlarged drawing shows that, when T_{error} is a constant, the value of ΔT depends on both the gradients of L_{AC} and L_{AB} . The slope of the full-heating curve decreases with increasing horizontal ordinate T . Thus, a great T_{sp} results in a small slope of L_{AC} , and a small D-value between ω_{sw} and ω_{sw}^* leads to a small ΔT . When T_0 is invariant, the overshoot T_{σ} therefore decreases with increasing T_{sp} . If WRC is set to start



Note: L_1 is the full-heating phase trajectory, L_2 is the self-heating phase trajectory, L_3 is the delay phase trajectory, Point A is the calculation switch point, Point C is the delay switch point

FIGURE 11. Graphical method for predicting the overshoot caused by the switching temperature error

when T_{sp} is greater than a constant C, then an upper bound T_{σ}^{\max} that satisfies $T_{\sigma} \leq T_{\sigma}^{\max}$ exists.

The overshoot of the WRC decreases with an increase in the variation of the set value. This is proof that WRC is more suitable to deal with wide changes in operating conditions rather than small changes.

4.3. Methods to determine which control scheme should be started. Based on the preceding analysis, this study produces two methods of on-line and off-line calculations for the switch judgment module to select WRC or regulatory PI control.

In Subsection 3.2, for the heating furnace model, when the initial temperature is 190 °C, the two control methods should be demarcated by 10 °C. That is to say, WRC should be started if the new set value is more than 200 °C; otherwise, the regulatory PI control is used. After verification, when the running condition is greater than 200 °C, we can still use 10 °C to select the control methods. For a simple object like this heating furnace model, calculating the switch conditions beforehand is the off-line calculation method.

Considering the extreme case when the temperature increases from 20 °C to 30 °C, the same ΔT_{sp} and T_{error} can result in an unacceptable overshoot, which is more than 2.5 °C. Consequently, we need another way to produce the starting threshold. If we let $\triangle ABC$ be a triangle in Figure 11 by approximating the curves L_{AC} and L_{AB} to straight segments and represent their slopes by k_{AC} and k_{AB} , respectively, then the on-line forecast can be simplified using some plane geometry knowledge. The specific calculation steps are as follows.

1) T_0 , T_{sp} and the object model are introduced into Equations (4) and (5) to compute the calculation switch point (T_{sw}, ω_{sw}) .

2) The values of k_{AC} and k_{AB} are obtained by taking (T_{sw}, ω_{sw}) in Equations (4) and (5), respectively.

3) The predictive value of the overshoot is $\Delta T = \left(1 - \frac{k_{AC}}{k_{AB}}\right) T_{error}$.

4) If the predictive value is within the allowed ranges, then WRC is selected for the start-up; conversely, the regulatory control is selected.

The on-line calculation method is suitable for objects that have a strong nonlinear property or wide running condition changes. Other targets with a weak nonlinear property or small changes can be satisfied by the off-line method, and the whole control process can also be simplified.

5. Comparison of the Performances of WRC and Regulatory Control. Continuous heating and cooling operations are implemented to the electric heating furnace model. The starting temperature is 20 °C. The set temperatures successively are 150 °C, 160 °C, 100 °C, 300 °C, 200 °C and 180 °C. As shown in Figure 12(a), the dotted line describes the effect of the regulatory control with invariant PI parameters, and the full line is the effect of WRC with the same PI parameters. When the new set value rises substantially, a satisfactory result may not be obtained using the PI control. However, when a large reduction occurs, the two control methods have a similar performance. This is due to the strong asymmetry of the heating furnace.

The comparison shows that, even when the non-optimal PI control parameters are used, the integrated control strategy with WRC as the supplementary scheme can maintain a good control effect on the whole working condition.

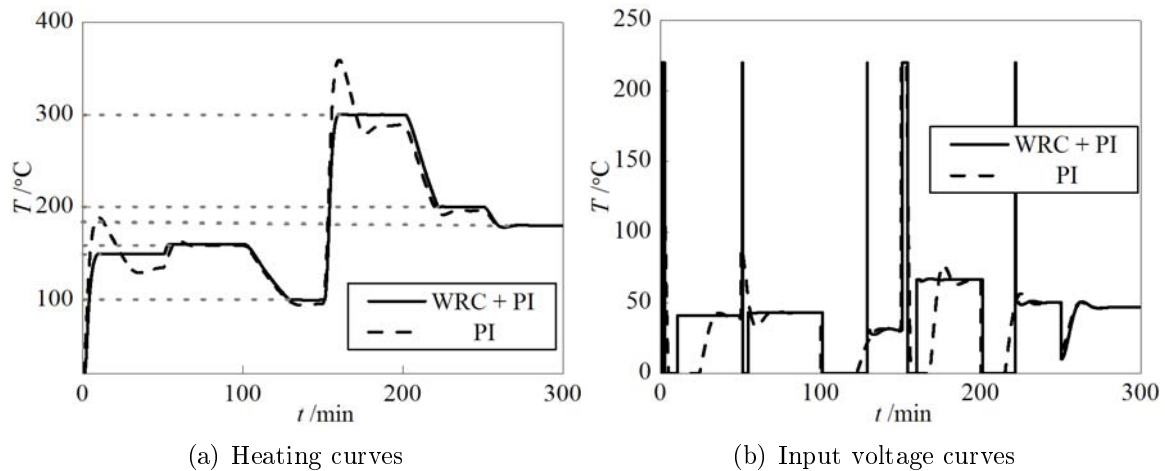


FIGURE 12. Comparison of control effects with continuous changes

6. Conclusions. Wide running condition changes are difficult to handle using regulatory control. Accordingly, we produce a control scheme called WRC-integrated Bang-Bang and regulatory control and design new calculation methods to solve the key problems and achieve better results. Firstly, the optimal switch point of Bang-Bang control is calculated as the intersection of phase curves by the phase locus graphic method. This method has the advantages of time controllability, high precision and online applicability. Secondly, we take the electric heating furnace as the object, from a brand new perspective, analyze the overshoot caused by the potential temperature measurement error and indicate the limitations of WRC in practical application. Contrasting WRC and regulatory control, we verify that their control performances are complementary. And based on the complementary feature, for different control objects, on-line and off-line methods are used to judge which control scheme should be started. The simulation result shows that the integrated strategy with WRC as supplement effectively solves the problem of excessively long regulation time or excessively large overshoot given wide changes in the running condition and meets the control requirements of the full range of operating conditions. In future work, we are determined to improve the integrated control strategy both in theory

and practice, especially extend the applicable range to high-order nonlinear systems and make it easy to implement in industrial control process.

Acknowledgment. This work was supported by the National Basic Research Program of China (2012CB720500). The authors also gratefully acknowledge the helpful comments and suggestions of the reviewers, which have improved the presentation.

REFERENCES

- [1] X. Guo, W. Du and R. Qi, Minimum time dynamic optimization using double-layer optimization algorithm. *The 10th World Congress on Intelligent Control and Automation*, Beijing, pp.87-88, 2012.
- [2] X. H. Yi, Q. Ye, L. Meng and R. Pei, The design and implementation of a rapid temperature control system, *Techniques of Automation and Application*, vol.18, no.3, pp.4-6, 1999.
- [3] Y. H. Zhang and Z. C. Zhang, A high-performance high-speed position orientation optimum system with low-cost based on Bang-Bang controller, *Power Electronics*, vol.37, no.1, pp.22-24, 2003.
- [4] H. Shibasaki, H. Ogawa and R. Tanaka, High speed activation and stopping control system using the Bang-Bang control for a DC motor, *IEEE Int. Symp. Ind. Electron.*, Taipei, Taiwan, pp.1-6, 2013.
- [5] L. P. Song, B. Liu and H. F. Chen, Approach to controlling the temperature of drying kiln using Bang-Bang adaptive fuzzy PID controller, *Comput. Appl. Chem. (China)*, vol.29, no.7, pp.121-124, 2012.
- [6] C. Y. Kaya and J. L. Noakes, Computations and time-optimal controls, *Optim. Contr. Appl. Met.*, vol.17, no.1, pp.171-185, 1996.
- [7] C. Y. Kaya and J. L. Noakes, Computational method for time-optimal switching control, *J. Optimiz. Theory. App.*, vol.117, no.1, pp.69-92, 2003.
- [8] X. L. Luo, Y. Ping and A. X. Feng, Multi-model intelligent switching control in uniform velocity process of electric heater, *Control Instrum. Chem. Ind.*, vol.37, no.11, pp.14-18, 2010.
- [9] X. L. Luo, R. X. Zuo and A. X. Feng, Modified switch control with buffer heating stage in chemical process startup, *J. Chem. Ind. Eng.*, vol.66, no.2, pp.647-654, 2015.
- [10] H. Q. Xiao, A intelligent control algorithm of engine speed based on soft-switching, *Automation & Instrumentation*, vol.25, no.4, pp.37-41, 2010.
- [11] Y. Zhou and C. Zhao, An iteratively adaptive particle swarm optimization approach for solving chemical dynamic optimization problems, *J. Chem. Ind. Eng.*, vol.65, no.4, pp.1296-1302, 2014.
- [12] Y. Ping and X. L. Luo, Human-simulated intelligent multi-model control of electric heater, *Control Instrum. Chem. Ind.*, vol.37, no.8, pp.30-33, 2010.
- [13] Y. Ke and F. R. Gao, Optimal start-up control of injection molding barrel temperature, *Polym. Eng. Sci.*, vol.47, no.3, pp.254-261, 2007.
- [14] S. S. Hu, *Automatic Control Theory*, Science Press, Beijing, 2007.